

In situ-Mercury Film Electrode for Simultaneous Determination of Lead and Cadmium Using Nafion Coated New Coumarin Schiff Base as Chelating-Adsorbent

Nelson Nuñez-Dallos¹, Carol Cuadrado², John Hurtado^{1,*}, Edgar Nagles^{2,*}, Olimpo García-Beltrán²

¹ Departamento de Química, Universidad de los Andes, Carrera 1 No. 18A-12, Bogotá, Colombia

² Facultad de Ciencias Naturales y Matemáticas, Universidad de Ibagué, Carrera 22 Calle 67, Ibagué, Colombia

*E-mail: edgar.nagles@unibague.edu.co, jj.hurtado@uniandes.edu.co

Received: 1 September 2016 / Accepted: 25 September 2016 / Published: 10 November 2016

Reaction of *o*-phenylenediamine and 8-formyl-7-hydroxycoumarin yield a new coumarin salen ligand, (CSB) which was isolated as orange air-stable solid and characterized by melting point, thermogravimetric analysis (TGA), mass spectra, infrared and NMR (¹H, ¹³C) spectroscopy. New CSB was dispersed in nafion and nafion-CSB composite was deposited on a glassy carbon electrode. The modified electrode nafion-CSB/GCE allowed the formation in-situ of mercury film for detection of Pb (II) and Cd(II) by anodic stripping voltammetry (ASV) in buffer phosphate solution pH 3.0 and 4.0. Optimal conditions were studied (mercury concentration: C_{Hg} 40.0 mg L⁻¹; CSB concentration; C_{CSB}; 20.0 μmol L⁻¹; pH 3.0 and pH 4.0; E_{ACC}: -1.1 V and t_{ACC}: 80). The detection limit (3σ/b) for Pb (II) Cd (II) were of 0.15 μg L⁻¹ for Pb(II) and Cd(II) at pH 3.0. Moreover, 0.071 and 0.080 μg L⁻¹ for Pb(II) and Cd(II), respectively at pH 4.0, The method was validated using ICP multi-element standard solution IX (Merck) containing As, Be, Cd, Cr(VI), Hg, Ni, Pb, Se and Tl 100 mg L⁻¹. Finally, river, tap and mineral waters were analyzed.

Keywords: Schiff base, 7-hydroxycoumarin, Anodic stripping voltammetry, Modified electrode, Lead, Cadmium, water samples

1. INTRODUCTION

Lead and cadmium are classified as hazardous metals by the Agency for Toxic Substances and Disease Registry. Excessive amounts of these metals in the environment is very harmful to humans, animals, and plants [1]. The contamination of lead and cadmium in living organism may cause irreparable damage to the DNA [2]. The water sources are the most affected ecosystem by the contamination of lead and cadmium from the industrial production. Therefore, is necessary the

developed of new sensitive methodologies that allow identifying and quantifying lead and cadmium in natural waters. Electroanalytical techniques offer great advantage, related to sensitivity and low operational costs. Anodic stripping voltammetry (ASV) has proven to be very effective to determine Pb and Cd; this is demonstrated by the numerous publications in the last decades. Modified carbon electrodes with bismuth [3], antimony [4] and mercury films [5], have been the most used methods to quantify lead and cadmium. Other alternatives have been the modification of electrodes with carbon nano-materials as graphene, [6], carbon nanotubes [7, 8], biological material such as bacteria [9] and ligands [10] as chelating-adsorbent agents. These chelating-adsorbent agents must form fast kinetic complexes and must be electro active. Moreover, the chelating-adsorbent agents must have active surface area (R-OH, R-O-R, etc.) that allow their spontaneous adsorption on the electrode surface. Some of the ligands used as chelating-adsorbent agents in the simultaneous determination of Pb and Cd are Clioquinol [11], 2-mercaptobenzothiazole [12], 8-hydroxyquinoline [13], 4-methylcatechol [14], uric acid [15], and pyrogallol red [16], where have been reported detection limits (DoL) between 0.05 and 17.0 $\mu\text{g L}^{-1}$ for lead and 0.01-10 $\mu\text{g L}^{-1}$ for cadmium. On the other hand, in these reports have using adsorptive stripping voltammetry (AdSV). Schiff bases are attractive as chelating-adsorbent agents in modified electrodes because of these ligands have the C=N donor system that can coordinate with various metal ions and form stable complexes. In addition, schiff bases are easy and inexpensive to prepare [17, 18, 19, 20, 21].

In this work, we report the synthesis of the Schiff base 8,8'-((1*E*,1'*E*)-(1,2-phenylenebis(azanylylidene))bis(methanylylidene))bis(7-hydroxy-2*H*-chromen-2-one) (Scheme 1). This new coumarin salen ligand can bind metal ions by the azomethine groups, as well as by the phenolic hydroxyl groups of the coumarin moieties. The aim of this research was to optimize the ASV technique to simultaneously determine Pb and Cd with mercury film and nafion coated new coumarin schiff base like chelating-adsorbent agent. To the best of our knowledge, *in-situ* mercury film electrodes with coumarin derivatives for the simultaneous determination of lead and cadmium have not been reported.

2. EXPERIMENTAL

2.1. Materials and methods

All reagents and solvents were used as received, without further purification. 7-hydroxycoumarin, hexamine, *o*-phenylenediamine, anhydrous magnesium sulfate, absolute ethanol, dichloromethane, acetonitrile, glacial acetic acid, nitric acid, among others, were of analytical grade and purchased from Merck. Cd(II), Pb(II), and Hg(II) standard solutions were prepared by diluting commercial standards (Merck). Water used for dilution of the standard, reagents, and preparation of samples was obtained from Merck (HPLC-type water). Nafion[®] (5% w/v solution) was obtained from Aldrich. All other chemicals such as nitric acid, KCl, etc., were analytical grade from Merck. Buffer phosphate solution (BPS) (0.1 mol L⁻¹) was prepared from H₃PO₄/H₂PO₄⁻/HPO₄²⁻, adjusting the pH

with NaOH solution. Reference ICP multi-element standard solution IX (Merck) containing As, Be, Cd, Cr(VI), Hg, Ni, Pb, Se and Tl 100 mg L⁻¹ was used for validation and interference studies.

The reactions were monitored by thin layer chromatography (TLC) on silica gel plates using dichloromethane or a mixture of dichloromethane and methanol (30:1) as solvents, and observed with UV lamp (254 nm or 365 nm). NMR data were recorded on a Bruker Avance 400 spectrometer (400.13 MHz for ¹H; 100.61 MHz for ¹³C). ¹H and ¹³C NMR chemical shifts δ are reported in parts per million (ppm) relative to TMS, with the residual solvent peak used as an internal reference. High resolution mass spectra (HRMS) were obtained on an Agilent Technologies Q-TOF 6520 spectrometer *via* an electrospray ionization (ESI) in positive ion mode. Infrared spectra (FT-IR) were recorded on a Thermo Nicolet Nexus 470 ESP FT-IR Spectrometer using KBr discs. Thermogravimetric analysis (TGA) was performed on a NETZSCH STA 409 PC/PG instrument in a nitrogen atmosphere with a continuous flow of 100 mL/min and a heating rate of 10 °C/min, from 30 to 700 °C. Melting points were determined in open capillary tubes on a Mel-Temp[®] Electrothermal melting point apparatus and are uncorrected.

SWASV's (square wave anodic stripping voltammograms) were obtained with a DropSens μ Stat 400 potentiostat. Electrochemical impedance spectroscopy (EIS) was obtained with a Versa Stat 3. potentiostat/galvanostat. Glassy carbon electrodes (3-mm) diameter, reference electrode Ag/AgCl/KCl 3 mol L⁻¹ and auxiliary electrode (platinum wire) were used. pH was measured with an Ohaus model ST 3100 pH meter.

2.2. Chemical synthesis and characterization

The coumarin Schiff base (**2**) was synthesized according to the Scheme 1. The synthetic procedure of 8-formyl-7-hydroxycoumarin (**1**) was adapted and slightly modified from literature [22].

2.2.1. Synthesis of 8-formyl-7-hydroxycoumarin (**1**)

A mixture of 7-hydroxycoumarin (5.0 g, 30.8 mmol), hexamine (10.0 g, 71.3 mmol) and glacial acetic acid (40 mL) was stirred at 95 °C for 5 h. Then aqueous 45% (v/v) HCl (80 mL) was added and the mixture was heated for 30 min. After the reaction mixture was cold down to room temperature, distilled water (400 mL) was added and the resulting solution was extracted with dichloromethane (5 x 100 mL). The combined organic extracts were washed with brine (250 mL), dried over anhydrous magnesium sulfate, filtered off and evaporated under reduced pressure to afford the crude product. Flash chromatography of the residue over silica gel, using dichloromethane, gave compound **1** as a pale yellow solid. Yield: 893 mg (15 %). mp 187-188 °C (from dichloromethane). $R_f = 0.3$ (DCM). IR (KBr, cm⁻¹): ν 3428, 3076, 2919, 1729, 1657, 1600, 1230, 1180, 1162, 1112, 997, 853. ¹H NMR (400 MHz, CDCl₃): δ (ppm) 12.21 (s, 1H), 10.60 (s, 1H), 7.65 (d, $J = 9.6$ Hz, 1H), 7.59 (d, $J = 8.8$ Hz, 1H), 6.89 (d, $J = 8.8$ Hz, 1H), 6.33 (d, $J = 9.6$ Hz, 1H). ¹³C NMR (100 MHz, CDCl₃): δ (ppm) 193.1 (HCO), 165.7 (C), 159.3 (C), 156.9 (C), 143.5 (CH), 136.1 (CH), 114.9 (CH), 113.6 (CH), 111.0 (C), 108.9 (C). HRMS (ESI+) m/z calculated for [C₁₀H₆O₄+H]⁺: 191.0339; found 191.0338 [M+H]⁺.

2.2.2. Synthesis of 8,8'-((1E,1'E)-(1,2-phenylenebis(azanylylidene))bis(methanylylidene))bis(7-hydroxy-2H-chromen-2-one) (2)

A solution of *o*-phenylenediamine (28.4 mg, 0.26 mmol) in ethanol (4 mL) was added dropwise to a solution of 8-formyl-7-hydroxycoumarin (100 mg, 0.52 mmol) in hot ethanol (7 mL), then the reaction mixture was stirred at 50 °C for 2 h. The compound **2** precipitated out as an orange solid. After TLC showed complete conversion, the reaction mixture was cold down to room temperature, and the precipitate was isolated by centrifugation, washed with cold ethanol and dried under vacuum. Yield: 113 mg (95 %). mp 241-242 °C (from ethanol). $R_f = 0.5$ (DCM:MeOH 30:1). IR (KBr, cm^{-1}): ν 3421, 3346, 1733, 1612, 1591, 1487, 1235, 1112, 834. ^1H NMR (400 MHz, CDCl_3): δ (ppm) 14.67 (s, 2H), 9.39 (s, 2H), 7.64 (d, $J = 9.5$ Hz, 2H), 7.45 (d, $J = 8.8$ Hz, 2H), 7.43 (m, 4H), 6.95 (d, $J = 8.8$ Hz, 2H), 6.26 (d, $J = 9.5$ Hz, 2H). ^{13}C NMR (100 MHz, CDCl_3): δ (ppm) 166.9 (C), 160.3 (C), 157.5 (CH), 155.4 (C), 144.2 (CH), 141.3 (C), 132.9 (CH), 128.9 (CH), 119.9 (CH), 115.7 (CH), 112.3 (CH), 110.3 (C), 107.3 (C). HRMS (ESI+) m/z calculated for $[\text{C}_{26}\text{H}_{16}\text{N}_2\text{O}_6+\text{H}]^+$: 453.1081; found 453.1109 $[\text{M}+\text{H}]^+$.

2.3. Anodic stripping voltammetry procedure

10 mL of water or 10 ml of sample, 250 μL Hg^{2+} solution 1000 mg L^{-1} , 200 μL of BPS (0.1 mol L^{-1}), and aliquots (10-100 μL) of Pb (II) and Cd(II) solutions (1.0 mg L^{-1}) were pipetted into the voltammetric cell, then, the pre-concentration step was initiated for an optimal time (t_{acc}) and potential (E_{acc}) at a stirring speed of 500 rpm. After an equilibration time of 3 s, SWASV's were recorded, while the potential was scanned from -1.1 to 0.0 V using square wave modulation with 10 mV step amplitude, 100 mV pulse amplitude and 30-Hz frequency. Each voltammogram was repeated three times. Calibration curves were obtained and detection limits (DL) were calculate from $3S_{x/y}/b$

2.4. Electrochemical impedance spectroscopy (EIS)

Electrochemistry Impedance Spectrum (EIS) was done with 10 mL of $\text{Fe}(\text{CN})_6^{3-}$ 0.01 mol L^{-1} in KCl 0.01 mol L^{-1} . Nyquist plot was obtained between 10.0 kHz and 1.0 Hz using glassy carbon electrode (GCE), glassy carbon coated nafion electrode (nafion-GCE) and glassy carbon coated nafion coumarin electrode (nafion-CSB/GCE).

2.5. Sample preparation

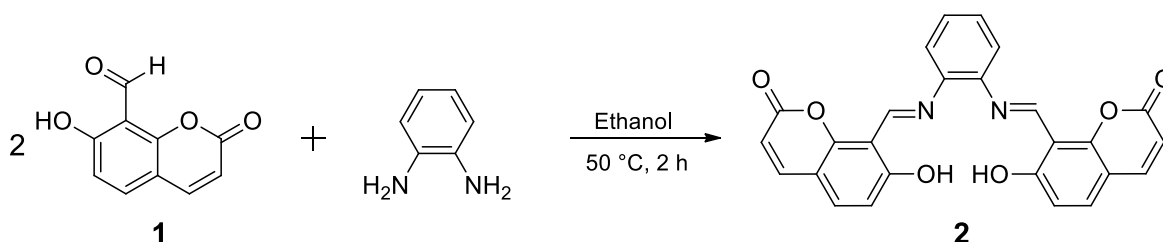
Commercial mineral water was bought from supermarket. River water samples were collected on August, 2016 from three points of the Ambala River, near to Universidad de Ibagué (Ibagué, Colombia). Tap water was obtained from our laboratory. Samples were stored frozen until analysis. Prior to analysis, the samples needed no treatment to remove organic matter. To eliminate matrix effects, the standard addition method was used. All measurements were obtained at room temperature (≈ 25 °C).

2.6. Preparation of in-situ mercury film nafion-coated new coumarin schiff base glassy carbon electrode (in-situ HgF-nafion-CSB/GCE)

Before each preparation, the GCE was polished with Al_2O_3 (0.05-0.3 μm) On a soft cloth, and submerged in a bath ultrasonic for five minutes with 0.3 mol L^{-1} HNO_3 and ethanol. 2.3 mg of CSB were mixed with 200 μL of nafion. After a strong agitation and when the mixture were homogenize, 10 μL were deposited on the electrode freshly polished to dryness of the excess solvent. nafion-coated new coumarin schiff base glassy carbon electrode (nafion-CSB/GCE) was developed. Mercury film was prepared in-situ. The electrode was immersed in an electro-analytical cell containing the plating solution of Hg(II) (30 mg L^{-1}) in the presence of Pb(II) and Cd(II) them, the mercury film was formed by holding the working electrode potential at -1.1 V for 80 s. No deaeration of the solutions was applied in this study. The entire study was performed with 10 mL of mercury dissolution.

3. RESULTS AND DISCUSSION

3.1. Synthesis of coumarin Schiff base



Scheme 1. Synthesis of coumarin Schiff base.

First, the reaction between 7-hydroxycoumarin and hexamine was carried out in glacial acetic acid to give 8-formyl-7-hydroxycoumarin **1**; this synthesis was adapted and slightly modified from literature [22]. Then, the coumarin Schiff base **2** was synthesized with a high yield (95%) from the condensation reaction between *o*-phenylenediamine and two equivalents of 8-formyl-7-hydroxycoumarin in absolute ethanol at 50 °C (Scheme 1). The compound was obtained as an orange solid with a melting point of 241-242 °C and showed low solubility in chloroform and dichloromethane. The molecular structure of new coumarin Schiff base was verified unambiguously by FT-IR, ^1H and ^{13}C NMR spectroscopy, and high resolution mass spectrum (HRMS) through electrospray ionization (ESI).

The IR spectrum showed a broad band at 3421 cm^{-1} corresponding to the $\nu(\text{O-H})$ stretching vibration of the phenolic OH bond. The strong band at 1733 cm^{-1} is assigned to $\nu(\text{C=O})$ stretching vibration of the carbonyl group in the lactone ring. An intense band at 1612 cm^{-1} corresponds to $\nu(\text{C=N})$ of the azomethine group.

The ^1H NMR chemical shift assignments of the coumarin Schiff base in CDCl_3 are shown in Figure 1. The singlet signal at lower field δ 14.67 can be attributed to the protons of phenolic OH

group, the downfield shift probably resulting from the intramolecular hydrogen bonding to the imine nitrogen. A singlet at δ 9.39 is due to azomethine proton (-N=C-H). There are two coupled doublets at δ 7.64 ($J = 9.5$ Hz) and δ 6.26 ($J = 9.5$ Hz) corresponding to the vinyl protons of the coumarin ring. The resonance shifts for aromatic protons are observed at δ 7.45-6.95. The integral values of the protons agree with the expected structure.

The HRMS (ESI+) spectrum in acetonitrile showed the ion peak $[M+H]^+$ at m/z 453.1109 (Calcd. 453.1081), which is consistent with the molecular weight of the ligand. The thermogravimetric analysis (TGA) curve in nitrogen atmosphere from 30 to 700 °C showed that the coumarin Schiff base has a decomposition temperature (T_{dec}) of 252 °C, which is defined as the temperature of 5% weight loss [23]. During the heating process, the TGA curve showed two stages of loss without formation of stable intermediates and with maximum decomposition rate at 312 and 515 °C. A total loss of 73.1% (Calcd. 71.7%) is observed in the temperature range of 200-700 °C, which is presumably due to the loss of two coumarin fragments.

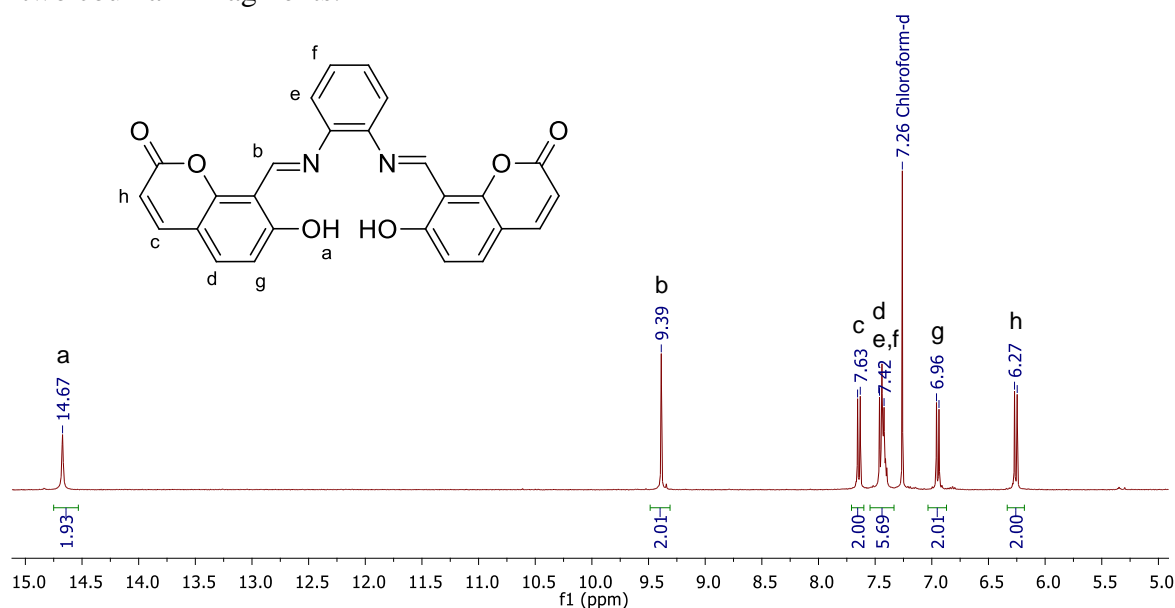


Figure 1. ^1H NMR spectrum of coumarin Schiff base in CDCl_3 .

3.1. Electroactive properties of nafion-CSB/GCE.

With the aim of verifying the electroactive properties of the new coumarin schiff base (CSB) in the modified electrode with nafion in regard to the transfer of electrons, was studied the modified surface using EIS. Results were reported in a Nyquist plot, with real resistance (Z') axis (x) is and imaginary resistance (Z'') axis (y) scanning of high to low frequencies. High resistance values while the frequency values decrease indicate a high impediment to the transfer of electrons [24]. Nyquist plot of a solution containing 0.01 mol L^{-1} of $\text{Fe}(\text{CN})_6^{3-}$ in $\text{KCl } 0.10 \text{ mol L}^{-1}$ on GCE, nafion/GCE and nafion-CSB/GCE are shown in Fig. 2. The graphic showed a semi-circle (curve a), using GCE in high frequency part between. This result suggests high impediment to the transfer of electrons. Using nafion/GCE (curve b) also suggest high impediment to the transfer of electrons. With nafion-

CSB/GCE (curve c), the values of z' resistance decreased considerably. Therefore, the transfer of electrons was improved when new coumarin was deposited on GCE with nafion.

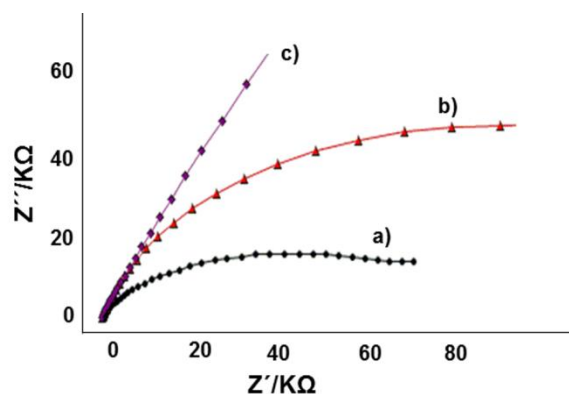


Figure 2. Nyquist plot of $0.01 \text{ mol L}^{-1} \text{Fe(CN)}_6^{-3}$ in $0.01 \text{ mol L}^{-1} \text{K}^{\text{Cl}}$ a) GCE, b) nafion/GCE and c) nafion-CSB/GCE.

3.2. Anodic stripping property of lead and cadmium on in-situ HgF-nafion-CSB/GCE

Preliminary experiments were performed to study the behavior of lead and cadmium on the modified electrode in-situ (*HgF-nafion-CSB/GCE*) in the presence of Hg (II) by ASV. When mercury solution is added to the cell, the film of mercury is formed in-situ at -1.1 V by 80 s allowing the reduction of lead and cadmium in the surface of the electrode.

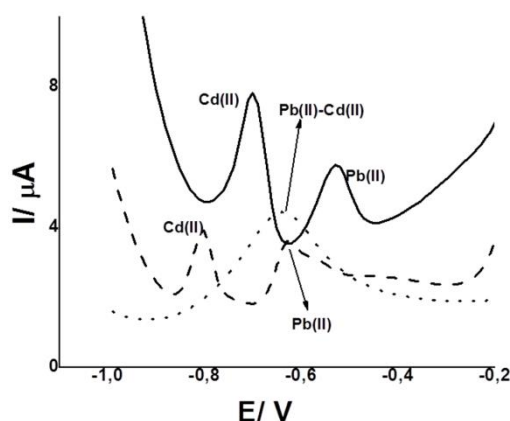


Figure 3. SWASV's of Pb(II) and Cd(II) ($4.7 \mu\text{g L}^{-1}$) using in-situ HgF/GCE (dot line), in-situ HgF-nafio /GCE (dash line) and in-situ *HgF-nafion-CSB/GCE* (solid line): Conditions: pH 3.0; $C_{\text{CSB}}: 24.17 \mu\text{mol L}^{-1}$; $C_{\text{Hg}}: 30 \text{ mg L}^{-1}$; $E_{\text{acc}}: -1.0 \text{ V}$; $t_{\text{acc}}: 60 \text{ s}$ step amplitude: 10 mV ; pulse amplitude: 50 mV and frequency: 20 Hz .

Figure 3 shows the oxidation of Pb (II) and Cd (II) $4.70 \mu\text{g L}^{-1}$ in the presence (solid line) and absence (dot and dash lines) of new coumarin (CSB) (30.2 mmol L^{-1}). In the absence of CSB, one

anodic peaks of Pb (II) and Cd (II) were seen at -0.64 V using in-situ HgF/GCE. Two well separated anodic peaks of Pb (II) and Cd (II) were seen at -0.67 and -0.81 V (anodic current 1.4 and 1.8 μA) respectively using in-situ HgF-nafion/GCE; whereas in the presence of CSB (in-situ HgF-nafion-CSB/GCE), two well-developed and separate anodic peaks to less negative potentials were seen (-0.54 and -0.71 V for Pb(II) and Cd(II), respectively), These signals confirm that the complexes have been formed and that requires more energy for Pb (II) and Cd (II) oxidation. Possibly the complex prevents the lead and cadmium penetrate very internally to the crystalline structure of mercury. Moreover, anodic peak currents increased, improving the charge transfer and sensitivity. With respect to the position of anodic peaks signals, *Hocevar et al.*, using antimony film [4], reported values of -0.53 and -0.78 V for Pb(II) and Cd(II), respectively, and *Wang et al.*, [3] using bismuth film reported values of -0.55 and -0.79 V for Pb(II) and Cd(II). In our measurements, peak currents were seen at similar potential.

3.3. Optimization of Operational Parameters

Aim to obtain the best conditions, peak currents for Pb(II) and Cd(II) using in-situ HgF-nafion-CSB/GCE were studied as a function of C_{Hg} , pH, C_{CSB} , E_{ACC} , and t_{ACC} . The results are shown below.

3.3.1. Study in function of the concentration of mercury (C_{Hg})

With the objective of decreasing the amount of mercury that is necessary for the formation of the film of mercury, has studied the anodic peak current for Pb (II) and Cd (II) on concentration of mercury between 10 - 40 mg L^{-1} (Fig. 4). The results showed that anodic peak currents for Pb (II) and Cd (II) were highest in 40 mg L^{-1} of Hg^{2+} .

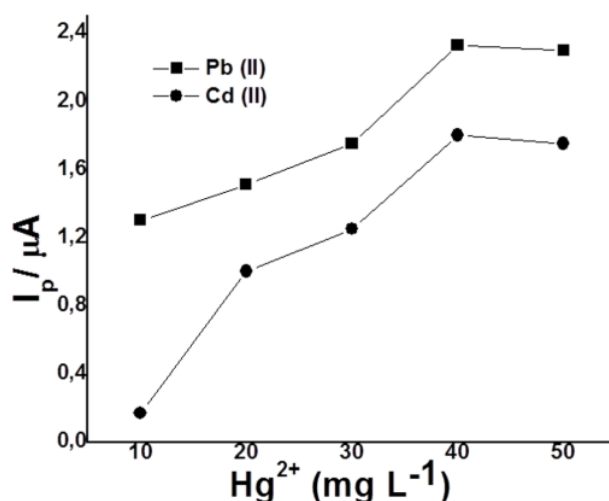


Figure 4. Peak currents for Pb(II) and Cd(II) in function of C_{Hg} using in-situ HgF-nafion-CSB/GCE Conditions: Pb(II), Cd(II) 4.7 $\mu\text{g L}^{-1}$. Other conditions as in Fig. 3.

3.3.2. Study in function of pH

The variation of anodic peak currents for Pb (II) and Cd (II) as a function of pH was studied using in-situ GC-HgF-NCM/E between 2.0 – 7.0 pH range (Fig. 5). Buffer compositions were $\text{H}_2\text{PO}_4^-/\text{H}_3\text{PO}_4$ (pH 2.0 – 4.0) and $\text{H}_2\text{PO}_4^-/\text{HPO}_4^{2-}$ (pH 5.0 - 7.0) solutions (0.1 mol L^{-1}). The conditions were: Pb (II) and Cd(II); $4.7 \text{ } \mu\text{g L}^{-1}$, C_{CSB} ; $24.17 \text{ } \mu\text{mol L}^{-1}$; C_{Hg} ; 30 mg L^{-1} $E_{\text{ACC}} = -1.0 \text{ V}$; and $t_{\text{ACC}} = 60 \text{ s}$.

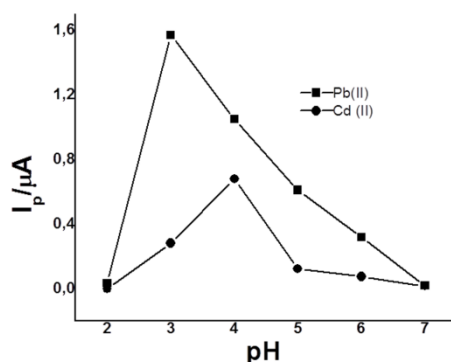


Figure 5. Peak currents of Pb(II) and Cd(II) in function of pH using in-situ HgF-nafion-CSB/GCE. Conditions: Pb(II), Cd(II) $4.7 \text{ } \mu\text{g L}^{-1}$. Other conditions as in Fig. 3.

The results showed that anodic peak currents was highest at pH 3.0 for Pb (II) and pH 4.0 for Cd (II). At pH 5.0, anodic peak currents decreased considerably. Metal hydroxide complexes can be formed with Pb (II) and Cd (II) and decrease anodic peak currents for at pH values higher of 5.0 [25]. Values of 3.0 and 4.0 were used for further experiments.

3.3.3. Study in function of the concentration of new coumarin (C_{CSB})

The CSB concentration is importance in relation with the sensitivity. C_{CSB} must to be at a concentration higher that concentration of Pb (II) and Cd (II); but excessive concentration could saturate the electrode surface, blocking the transport of charge, affecting sensitivity. Anodic peak currents for Pb (II) and Cd (II) increased with increasing C_{CM} up to $\sim 20.0 \text{ } \mu\text{mol L}^{-1}$ and then decreased considerably, probably because the free C_{CSB} saturate the electrode surface. An optimum CM concentration of $20.0 \text{ } \mu\text{mol L}^{-1}$ was used for further experiments.

3.3.4. Influence of E_{ACC} and t_{ACC} on the anodic peak currents.

Accumulation potential (E_{ACC}) on the peak currents was studied over the -1.4 to -1.0 V range in presence of Pb(II) and Cd(II) $4.7 \text{ } \mu\text{g L}^{-1}$. Anodic peak currents were maximum for Pb (II) and Cd(II) at -1.4 V. However, the stability of the electrode surface was affected, possibly by the hydrolysis of water. An E_{acc} of -1.1 V was chosen for further studies. Another parameter studied was accumulation time (t_{ACC}), this was examined in 10–110 s range. Anodic Peak currents for Pb (II) and Cd (II)

increased linearly with time accumulation until 80 s, and then tended to a constant value. The value of 80 s was used for further studies.

3.4. Effect of instrumental variables (frequency, step potential, and amplitude)

Instrumental parameters provide a portion of the sensitivity and selectivity. The instrumental parameters studied were: frequency, step amplitude, and pulse amplitude. Anodic peak currents increased as all parameters increased. Frequency of 20 Hz, step amplitude of 10 mV and pulse amplitude of 50 were selected for further experiments.

3.5. Detection limit (DL) and reproducibility (% RSD).

LD and % RSD using optimal conditions (C_{Hg} ; 40.0 mg L⁻¹, C_{CSB} ; 20.0 μmol L⁻¹ pH 3.0 for Pb (II) and pH 4.0 for Cd(II) (PBS); E_{ACC} : -1.1 V and t_{ACC} : 80 s with stirring rate 500 rpm; step amplitude 10 mV; pulse amplitude 500 mV, and frequency of 20 Hz) using in-situ HgF-nafion-CSB/GCE were obtained. Anodic peak currents were proportional to the concentration of Pb(II) and Cd(II) over the 0.95–10.5. μg L⁻¹ range, with a detection limit ($3S_{x/y}/b$) of 0.15 μg L⁻¹ for Pb(II) and Cd(II) at pH 3.0 (Fig. 6A) and 0.071 and 0.080 μg L⁻¹ for Pb(II) and Cd(II), respectively (Fig. 6B) at pH 4.0. The results showed that the current ratio between the Pb (II) and Cd (II) is almost 1:1 and the sensitivity is improved at pH 4.0. The relative standard deviations were 1.0% and 1.5% for Pb(II) and Cd(II), respectively, ($n = 7$) for solutions containing Pb(II) and Cd(II) 4.70 μg L⁻¹. The results obtained were equally acceptable to other work previously with antimony [4] and bismuth [3]film electrodes. The table 1 summarize other modified electrodes using for Pb and Cd.

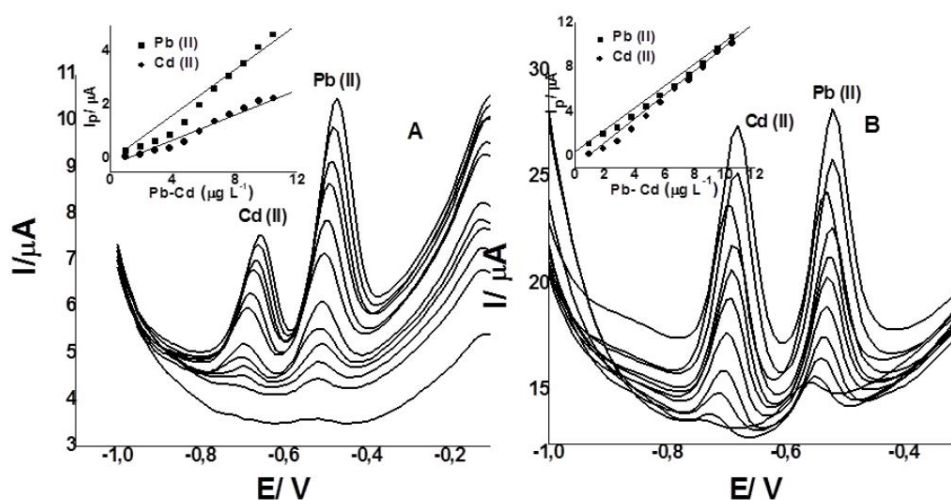


Figure 6. SWASV's and calibration curve (insert) for increasing concentration of Pb(II) and Cd(II) A) pH 3.0 and B) pH 4.0 using in-situ HgF-nafion-CSB/GCE. Conditions: C_{Hg} ; 40.0 mg L⁻¹; C_{CSB} 20.0 μmol L⁻¹; E_{ACC} -1.1 V; t_{ACC} 80s. Other conditions as in Fig. 3.

Table 1. Detection limit for Pb(II) and Cd (II) using modified electrodes.

Electrode	Material	Detection limit ($\mu\text{g L}^{-1}$)		References
		Pb	Cd	
SPCE	Bi-PSS	0.27	0.10	[26]
GCE	BiOCl/MWCNT	1.90	4.00	[27]
SPCE	N/IL/G	0.08	0.06	[28]
GCE	NG	0.050	0.56	[29]
GCE	HgF-N-CSB	0.071	0.080	This work

SPCE: screen printed carbon electrode; Bi: bismuth; PSS: polystyrene sulfonate; BiOCl: bismuth-oxochloride; MWCNT: multi walled carbon nanotubes; N/IL/G: nafion/ionic liquid/graphene; NG: N-doped graphene; HgF: mercury film; CSB; coumarin salen ligand.

3.6. Validation of the method and interference study

The accuracy and interferences of the method was evaluated by determining Pb(II) and Cd(II) using ICP multi-element standard solution IX (Merck) containing As, Be, Cd, Cr(VI), Hg, Ni, Pb, Se and Tl 100 mg L^{-1} . The results have been summarized in table 2. Standard solution was diluted to 1 mg L^{-1} and $50 \mu\text{L}$ were added to the cell with 10 mL of water, 0.25 mL BPS and 0.25 mL Hg^{2+} . These results were satisfactory because the standard tested contains other metal ions that could interfere with the signals of Pb (II) and Cd (II).

Table 2. Values obtained for Pb and Cd using ICP multi-element standard solution. (n=3) using in-situ HgF-nafion-CSB/GCE

Standar solution ($\mu\text{g L}^{-1}$)		Found ($\mu\text{g L}^{-1}$)		% Relative error	
Pb (II)	Cd(II)	Pb (II)	Cd(II)	Pb (II)	Cd(II)
4.76	4.76	4.58	6.00	-3.78	26.0
4.76	4.76	5.60	4.37	17.6	-8.19

3.7. Analysis of real samples

in-situ HgF-nafion-CSB/GCE was used to determine Pb(II) and Cd(II) in commercial mineral, tap and river waters without prior treatment. The results have been summarized in table 3. Cd(II) was not detected in any of these samples. possibly the concentration is lower than the detection limited. Similar results have been reported previously for the same type of samples using mercury film electrode [26].

Table 3. Values obtained for Pb and Cd in real samples (n=2) using in-situ HgF-nafion-CSB/GCE

Waters samples	Found ($\mu\text{g L}^{-1}$)	
	Pb (II)	Cd (II)
Mineral	1.73	-
Mineral	2.1	0.12
*River (Ambala)	1.8	0.084
River (Ambala)	0.9	0.38
Tap	0.22	0.21

*Figure 7 show voltammograms and calibration curve (insert) for Ambala river

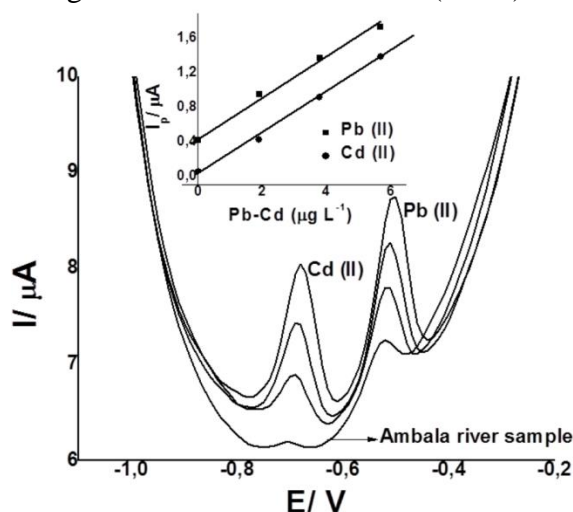


Figure 7. SWASV's and calibration curve (insert) for *Ambala river sample using in-situ HgF-nafion-CSB/GCE. Conditions: pH 4.0; C_{Hg} ; 40.0 mg L⁻¹; C_{CSB} 20.0 $\mu\text{mol L}^{-1}$; E_{ACC} -1.1 V; t_{ACC} 80s. Other conditions as in Fig. 3.

4. CONCLUSIONS

In summary, we have developed an *in situ* mercury film nafion coated electrode for the simultaneous determination of Pb(II) and Cd(II) using a new coumarin salen ligand as chelating-adsorbent. This ligand was synthesized efficiently by a simple Schiff base condensation between *o*-phenylenediamine and 8-formyl-7-hydroxycoumarin. The accumulation step was more effective with the new coumarin, allowing greater sensitivity. Analysis of the real samples does not need pretreatment optimizing the analysis time.

ACKNOWLEDGEMENTS

E.O, C.C and O.B are gratefully acknowledged to financial support from Universidad de Ibagué (15-343-INT and 15-376-INT). Thanks to the Department of Chemistry and the School of Science of the Universidad de los Andes for the financial support. NND is also grateful to COLCIENCIAS for his doctoral scholarship (Conv. 617). The authors would like to thank Andrés Posada for his assistance in the research.

References

1. M. Krawczyk, M. Jeszka, *Microchem. J.*, 126 (2016) 296.
2. V. Matović, A. Buha, D. Đukić-C'osic', Z. Bulat, *Food Chem., Toxicol.*, 78 (2015) 130.
3. J. Wang, J. Lu, B. Hocevar, A. Percio, M. Farias, *Anal. Chem.*, 72 (2001) 3218.
4. S. B. Hocevar, I. Švancara, B. Ogorevc, K. Vytras, *Anal. Chem.*, 79 (2007) 8639.
5. J.E. Poldoski, G.E. Glass, *Anal. Chim. Acta.*, 101 (1978) 79.
6. J. Shan, Y. Liu, R. Li, C. Wu, L. Zhu, J. Zhang, *J. Anal. Chem.*, 738 (2015) 123.
7. S. J. Prabakar, C. Sakthivel, S. Sriman, *Talanta*. 85 (2011) 290.
8. S. Cerovac, V. Guzsány, Z. Kónya, M. Ashrafi, I. Švancara, S. Rončević, Á. Kukovecz, B. Dalmacija, K. Vytrás, *Talanta*. 134 (2015) 640.
9. B. Kong, B. Tang, X. Liu, X. Zeng, H. Duan, S. Luo, W. Wei, *J. hazard Mater.*, 167 (2009) 455.
10. O. Hernández, I. Rodríguez, J. L. Hidalgo, E. Reguera, *Sensor Actuat., B-Chem.*, 123(2007) 488.
11. E. Herrero, V. Arancibia, C. Rojas, *J Electroanal., Chem.*, 729 (1993) 9.
12. S. Abbasi, K. Khodarahmiyan, F. Abbasi, *Food Chem.*, 128 (2011) 254.
13. C. Colombo, C.M.G. van den Berg, *Anal. Chim. Acta* 337 (1997) 29.
14. J. Limson, T. Nyokong, *Anal. Chim. Acta* 344 (1997) 87.
15. A. Gandour, E. A. Kasim, A.H. Amrallah, O.A. Farghaly. *Talanta.*, 41 (1994) 439.
16. E. Nagles, V. Arancibia, C. Rojas, R. Segura, *Talanta*. 99 (2012) 119.
17. M. R. Ganjali, M. Tavakoli, F. Faridbod, S. Riahi, P. Norouzi, M. Salavati-Niassari, *Int. J. Electrochem. Sci.*, 3 (2008) 1559.
18. J. Qin, L. Fan, T. Li, Z. Yang, *Synth. Met.*, 199 (2015) 179.
19. Y. Dong, J. Li, X. Jiang, F. Song, Y. Cheng, C. Zhu, *Org. Lett.*, 13 (2011) 2252.
20. J. Orrego-Hernández, N. Nuñez-Dallos, J. Portilla, *Talanta*, 152 (2016) 432.
21. S. Patil, S. Unki, P. Badami, *J. Therm. Anal. Calorim.* 111 (2013) 1281.
22. M. Black, J. I. G. Cadogan, H. McNab, A. D. MacPherson, V. P. Roddam, C. Smith, H. R. Swenson, . *J. Chem. Soc. Perkin Trans. 1*, 42 (1997) 2483.
23. F. Wu, J. Li, H. Tong, Z. Li, C. Adachi, A. Langlois, P. D. Harvey, L. Liu, W.-Y. Wong, W.-K. Wong, X. Zhu, *J. Mater. Chem. C*, 3 (2015) 138.
24. A. Ensafi, B. Arashpour, B. Rezaei, A. Allafchian, *Mat. Sci. Eng., C-Biomim.*, 39 (2014) 78.
25. S. Lee, S. Park, E. Choi, Y. Piao, *J. Electroanal. Chem.*, 766 (2016)120.
26. R. Maria-Hormigos, M. Gismera, J. R. Procopio, M. Sevilla, *J. Electroanal. Chem.*, 767 (2016) 114.
27. S. Cerovac, V. Guzsány, Z. Kónya, A. M. Ashrafi, I. Švancara, S. Rončević, Á. Kukovecz, B. Dalmacija, K. Vytrás. *Talanta* Volume 134 (2015) 640.
28. S. Chaiyo, E. Mehmeti, K. Žagar, W. Siangproh, O. Chailapakul, K. Kalcher, *Anal. Chim. Acta*. 918 (2016) 26.
29. H. Xing, J. Xu, X. Zhu, X. Duan, L. Lu, W. Wang, Y. Zhang, T. Yang. *J. Electroanal. Chem.*, 760 (2016) 52.
30. E. Herrero, V. Arancibia, C. Rojas–Romo. *J. Electroanal. Chem.*, 729 (2014) 9.